Efficient Gene Delivery and Expression in Pancreas and Pancreatic Tumors by Capsid-Optimized AAV8 Vectors

Min Chen,[1,†,‡] Kyungah Maeng,[1,†] Akbar Nawab,[1] Rony A. Francois,[1] Julie K. Bray,[1] Mary K. Reinhard,[2] Sanford L. Boye,[3] William W. Hauswirth,[3] Frederic J. Kaye,[4] Georgiy Aslanidi,[5] Arun Srivastava,[5] and Maria Zajac-Kaye[1,*]

Departments of [1]Anatomy and Cell Biology, [2]Veterinary Medicine, [3]Ophthalmology, and [4]Medicine and [5]Division of Cellular and Molecular Therapy, Department of Pediatrics, University of Florida College of Medicine, Gainesville, Florida.

[†]*These authors contributed equally to this work.*

[‡]*Current address: Changjiang Scholar Laboratory, Shantou University Medical College, Shantou, Guangdong, China.*

Despite efforts to use adeno-associated viral (AAV) vector–mediated gene therapy for treatment of pancreatic ductal adenocarcinoma (PDAC), transduction efficiency remains a limiting factor and thus improvement of AAV delivery would significantly facilitate the treatment of this malignancy. Site-directed mutagenesis of specific tyrosine (Y) residues to phenylalanine (F) on the surface of various AAV serotype capsids has been reported as a method for enhancing gene transfer efficiencies. In the present studies, we determine whether Y-to-F mutations could also enhance AAV8 gene transfer in the pancreas to facilitate gene therapy for PDAC. Three different Y-to-F mutant vectors (a single-mutant, Y733F; a double-mutant, Y447F+Y733F; and a triple-mutant, Y275F+Y447F+Y733F) and wild-type AAV8 (WT-AAV8) were administered by intraperitoneal or tail-vein routes to $Kras^{G12D+/-}$, $Kras^{G12D+/-}/Pten^{+/-}$, and wild-type mice. The transduction efficiency of these vectors expressing the mCherry reporter gene was evaluated 2 weeks post administration in pancreas or PDAC and correlated with viral genome copy numbers. Our comparative and quantitative analyses of the transduction profiles demonstrated that the Y-to-F double-mutant exhibited the highest mCherry expression in pancreatic tissues (range 45–70%) compared with WT-AAV8 (7%; $p < 0.01$). We also detected a 7-fold higher level of vector genome copy numbers in normal pancreas following transduction with the double-mutant AAV8 compared with WT-AAV8 (10,285 vs. 1,500 vector copies/μg DNA respectively, $p < 0.05$). In addition, we observed that intraperitoneal injection of the double-mutant AAV8 led to a 15-fold enhanced transduction efficiency as compared to WT-AAV8 in mouse PDAC, with a corresponding $\sim$14-fold increase in vector genome copy numbers (26,575 vs. 2,165 copies/μg DNA respectively, $p < 0.05$). These findings indicate that the Y447+Y733F-AAV8 leads to a significant enhancement of transduction efficiency in both normal and malignant pancreatic tissues, suggesting the potential use of this vector in targeting pancreatic diseases in general, and PDAC in particular.

Keywords: gene therapy, pancreatic cancer, adeno-associated virus, AAV8

INTRODUCTION

PANCREATIC DUCTAL ADENOCARCINOMA (PDAC) shows a rapid clinical course with a median survival of 6 months and a 5-year survival rate of only 3%.[1,2] PDAC responds poorly to conventional therapies, including chemotherapy and irradiation. Surgery is possible only in 10–20% of the patients due to extensive invasion of surrounding structures at the time of diagnosis.[3,4] The incidence of pancreatic cancer has increased over the last four decades,[5] indicating a pressing need for effective strategies against pancreatic cancer.[6,7] Several studies reported the development of recombinant adeno-associated virus (AAV)–mediated gene therapy for PDAC.[8,9] For example, AAV2-mediated expression of endostatin-inhibited tumor growth and metastasis in an orthotopic pancreatic cancer model[8] and AAV2-mediated *snail* siRNA inhibited the growth of pancreatic tumor xenograft.[9] From these studies, systemic gene therapy appears to be

*Correspondence: Maria Zajac-Kaye, PhD, University of Florida, UF Health Cancer Center, 2033 Mowry Rd, R360, Gainesville, FL 32610. E-mail: mzajackaye@ufl.edu

DOI: 10.1089/hgtb.2016.089

effective for both inhibiting tumor growth and preventing metastases in PDAC models.[8,9] Moreover, these reports have opened new avenues for the efficient management of pancreatic malignancy using AAV-integrated gene therapy technology.[8,9]

AAV vectors are recognized as a safe and effective delivery system for gene therapy due to a number of favorable features including lack of pathogenicity, low immunogenicity, lack of viral coding sequences, broad tropism, and the ability to support strong and persistent transgene expression.[10,11] Thus far, 12 serotypes of AAV (AAV1 to AAV12) have been studied extensively as gene therapy vectors.[12] Various AAV serotype vectors have been successfully applied in over 100 clinical trials with an excellent safety profile.[13,14] Among the various serotypes, AAV8 is particularly attractive as a gene therapy vector due to its higher transduction efficiency than other serotype (10- to 100-fold) and lower level of preexisting neutralizing antibodies.[15–17] Furthermore, AAV8 crosses vascular endothelial barriers more efficiently than other serotypes, resulting in efficient gene delivery to hepatic, cardiac, and skeletal muscle cells.[18,19] The first successful AAV8-mediated gene transfer has been achieved in patients with hemophilia B.[20] AAV8 also shows modest transduction of normal exocrine and endocrine pancreas when delivered systemically,[21,22] intrapancreatically,[23,24] intraductally,[22,25] or through the intrapancreatic vessels in animal models.[26] The remaining obstacles for pancreatic tropism includes, irrespective of the serotype employed, the persistence of vector dose-dependent immune response and the modest level of transduction efficacy.[27,28]

A major barrier for AAV gene therapy is the degradation of viral particles during their intracellular trafficking via the ubiquitination-proteasomal degradation machinery.[29] To evade phosphorylation and subsequent ubiquitination leading to vector loss, capsid-optimized AAV vectors were developed using site-directed tyrosine to phenylalanine (Y-F) mutagenesis of one or more of the seven surface-exposed tyrosine residues in the viral protein 3 common region of the capsid.[30] These Y-F mutant vectors have been reported to protect vector particles from proteasome degradation and yield significant increases in the transduction efficiency of mutant vectors relative to their wild-type (WT) counterparts.[30] For example, AAV1, AAV2, AAV3, AAV6, AAV8 or AAV9 containing single or multi-Y-F point mutation sites of the surface-exposed tyrosine residues are significantly more efficient in transducing cells and tissues such as human hematopoietic stem cells, retina, muscle, lung, and liver.[30–34] Following these discoveries, capsid mutant AAV vectors have been investigated in proof-of-concept studies for gene therapy in animal models and have been shown to provide long-term retinal preservation,[35] correction of murine hemophilia B,[36] and restoration of pyruvate dehydrogenase complex activity.[37] More recently, the safety and efficacy of capsid-optimized AAV serotype vectors have also been documented in non-human primates[38] and human phase 1 clinical trial.[14,20,39]

In the current study, we used capsid-optimized AAV8 Y-F mutant vectors to promote high transduction efficiency of gene delivery in normal pancreatic tissue and PDAC. We report that a single intraperitoneal administration of a double tyrosine mutant AAV8 (Y447F+Y733F) at a relatively low dose [$1–3\times10^{11}$ viral genomes per animal (vg/animal)] exhibits robust transgene expression in normal and malignant mouse pancreas.

MATERIALS AND METHODS

Site-directed mutagenesis of AAV8 mutant capsids

Tyrosine (Y) to phenylalanine (F) mutant AAV8 capsid were generated by site-directed mutagenesis,[40] in a manner similar to previously described generation of AAV2 tyrosine mutants.[30] Briefly, Y275F, Y447F, and Y733F mutations were introduced in the pAAV8 capsid plasmid[40] using a Multi Site-Directed Mutagenesis Kit (Stratagene, Agilent Technologies, La Jolla, CA) according to the manufacturer's protocol. Selected tyrosine residues were mutated to phenylalanine to generate the following vectors: a single mutant, Y733F; a double mutant, Y447F+Y733F; and a triple mutant, Y275F+Y447F+Y733F. Phenylalanine was chosen due to similarity in size, opposite charge, and lack of recognition by cellular kinases.[29] The presence of the desired point mutation was verified by restriction enzyme analysis and DNA sequencing (Applied Biosystems 3130 Genetic Analyzer; Life Technologies, Warrington, United Kingdom). The amino acids on AAV8 capsid are numbered according to the National Center for Biotechnology Information database (accession ID: NC_006261.1).

Generation of recombinant AAV

In this study, we used AAV2 genomes pseudotype only in AAV8 capsids, and not in AAV2 capsids; thus the same AAV2 genomes were encapsidated in WT as well as in the mutant AAV8 capsids. A self-complementary (sc) AAV8 vector encoding a red fluorescent protein mCherry (sc-smCBA-mCherry) that is driven by the small chicken β-actin (CBA) promoter has been previously described.[41] The AAV8 mutant capsids were packaged, purified, and titered

according to previously described methods.[42] Briefly, recombinant AAV (rAAV) vectors were generated by transient transfection of HEK293T cells using three AAV plasmids (pAAV8-rep/cap-wild type or pAAV8-rep/cap-Y-F mutant, sc-smCBA-mCherry and pHelper).[42,43] HEK293T cells were transiently transfected at 80% confluency in forty 150-mm^2 dishes using 20 mL of polyethylenimine (linear, MW 25,000, Polysciences, Inc.). Cells were collected 72 hours post-transfection, lysed, and treated with 25 units/mL of benzonase nuclease (Sigma Aldrich, Louis, MO). Subsequently, the recombinant AAV were purified by iodixanol step-gradient ultracentrifugation (Optiprep, Sigma Aldrich), followed by column chromatography (HiTrap Q column, GE Healthcare, Pittsburgh, PA). Recombinant AAV vectors were then concentrated to a final volume of 0.5 ml in phosphate buffered saline using Amicon Ultra 10K centrifugal filters (Millipore, Bedford, MA). The viral DNA-containing AAV vector titers were quantified by real-time PCR analysis and expressed as viral genomes per milliliter (vg/mL). PCR primer sets specific for CBA promoter have been previously described.[42,43] A 10-fold dilution series of the control plasmid DNA (sc-smCBA-mCherry) was used to generate standard curve, and AAV signal was compared with the standard curve to determine the AAV vector genome titer. After viral titration, AAV were aliquoted and stored at –80°C until used.

Animals

To generate *Pdx1-Cre*$^+$, *Kras*$^{G12D/+}$, and *Pten*$^{lox/+}$ mice, we backcrossed the *Kras*$^{G12D/+}$ line (on a B6.129 background, NCI Mouse Repository No. 01XJ6) to the *Pten*$^{lox/+}$ mice (on a 129/BALB/c background, Jackson lab No. 004597). We then crossed *Kras*$^{G12D/+}$;*Pten*$^{lox/+}$ mice to *Pdx1-Cre*$^+$ mice (on a B6/FVB background, NCI Mouse Repository No. 01XL5).[44] All experimental mice (FVB/C129; *Pdx1-Cre*$^+$, *Kras*$^{G12D/+}$, and *Pten*$^{lox/+}$) were housed and handled at the University of Florida Animal Facility. All experiments were approved by the Institutional Animal Care and Use Committee at the University of Florida.

Recombinant AAV8 transduction studies *in vivo*

WT and Y-F mutant AAV8 (WT-AAV8 and Y447F+Y733F-AAV8) were administered via the tail vein or intraperitoneal (i.p.) injection into 2-month-old FVB/C129 mice at a dose of 1×10^{11} vg/animal. Mice were euthanized 2 weeks after AAV administration. Mouse tissues were assessed for mCherry expression either by *ex vivo* imaging or by fluorescence microscopy as described in sections below. Additionally, WT and Y447F+Y733F-AAV8 were intraperitoneally administered at a dose of 3×10^{11} vg/animal into 2-month-old Kras$^{G12D/+}$/Pten$^{+/-}$ or 5-month-old Kras$^{G12D/+}$ mice. Two weeks after AAV injection, examination of mCherry expression and viral genome copy number on normal or tumor tissues was performed following euthanasia (see below).

Examination of mCherry expression

Ex vivo visualization of mCherry was performed in different organs as follows. Internal organs were collected, placed on black paper (Artagain black paper, Strathmore cat No. 445-109), and the fluorescence intensity was measured using IVIS Imaging System (Caliper Life Sciences, Hopkinton, MA). *In vivo* imaging system (IVIS) data are presented as radiant efficiency [(p/s/cm^2/sr)/(μW/cm^2)]. Radiant efficiency is the number of photons (p) per second (s) that leave a square centimeter (cm^2) of tissue and radiate into a solid angle of one steradian (sr) normalized to the incident excitation intensity (μW) per square centimeter. Quantification of fluorescent signals from organs was analyzed by Living-Image 4 software (Caliper Life Sciences).

Cross-sections from liver and pancreas were used to assess mCherry expression by a fluorescence microscope (Leica CTR6000; Leica Microsystems GmbH, Stuttgart, Germany). Briefly, individual organs were collected, fixed in 4% paraformaldehyde for 24 hours, immersed in 30% sucrose for 24 hours, mounted in optimal cutting temperature (OCT) medium (Tissue-Tek, Torrance, CA), and snap frozen. Cryosections were cut (Leica, Cryostat CM30505) and mounted in DAPI-containing fluorescence mounting media (Invitrogen Molecular Probes, Eugene OR). Fluorescent images of cryosection were recorded using an Olympus DP70 digital camera coupled to an Olympus IX71 inverted microscope (Olympus Corp, Japan). Fluorescence expression efficiency was measured using Image J software.

Real-time PCR for AAV genome copy number determination

At necropsy, the pancreas and liver were frozen in OCT medium and stored at –80°C until genomic DNA was extracted. Total DNA was extracted with a DNAeasy Blood and Tissue kit (Qiagen, Valencia, CA). Vector genome copy number was determined with a 7900 HT real-time PCR system (Applied Biosystems, Foster City, CA). TaqMan assays for viral vector genome copy number were developed using primers and probe for the CBA promoter region. Forward primer is TCTGCTTCACTCTCCC

CATCTC. Reverse primer is CCATCGCTGCACA AAATAATTAAA. Fluorescent probe is 6FAM (6-carboxyfluorescein)-CCCCCTCCCCACCCCCAATT. sc-smCBA-mCherry plasmid[42,43] was used to produce a standard curve. PCR reactions contained a total volume of 100 μL and were run under the following conditions: 50°C for 2 minutes, 95°C for 10 minutes, 45 cycles of 95°C for 15 seconds, and 60°C for one minute. DNA samples were assayed in triplicate. In order to rule out false negatives due to PCR inhibition by viral DNA, the third replicate was "spiked" with positive control plasmid DNA (sc-smCBA-mCherry) at a concentration of 100 copies/g of total genomic DNA. The AAV vector genome copy number is normalized as viral genomes copy number per μg of total genomic DNA. AAV vector genome copy number determination procedures were performed at the Powell Gene Therapy Center Vector Core facility at University of Florida.

Statistical analysis

A two-tailed Student's *t*-test determined probability of difference. A p value <0.05 was considered significant. Statistical analyses were performed using Prism 6.0 (GraphPad Software).

RESULTS

Y-F mutants of AAV8 transduce the mouse pancreas more efficiently than WT AAV8

Studies demonstrated that Y-F mutation in AAV2 and AAV3 capsids facilitate viral nuclear transport by limiting proteasome-mediated degradation, leading to high-efficiency transduction.[30,31,45,46] In addition, capsid-optimized AAV8 vectors recently showed great improvement in transduction efficiency in mouse retina and brain.[47,48] Because AAV8 has previously been shown to target pancreatic tissues,[22,49] we tested three next-generation AAV8 Y-F mutant (M) vectors (1M, Y733F; 2M, Y447F+Y733F; or 3M, Y275F+Y447F+Y733F) to determine whether these three AAV8 capsid mutants increase transduction efficiency in the pancreas (Table 1). Wild-type and three capsid Y-F mutant AAV8 were administered i.p. to FVB/C129 mice at a dose of 1×10^{11} vg/animal. Tissues were collected 2 weeks after injection to allow enough time for sufficient AAV mediated gene expression,[50,51] and mCherry fluorescent intensity was measured to compare the *in vivo* tropism profile of AAV8 Y-F capsid mutants to WT-AAV8. *Ex vivo* tissue fluorescence imaging of the mCherry signal revealed the WT-AAV8 vector efficiently transduced predominantly in the liver (average 2.46×10^{10} radiant efficiency) with 10-fold less signal in the pancreas (average 2.32×10^{9} radiant efficiency) (Fig. 1A).

Table 1. *Nomenclature of capsid-optimized tyrosine to phenylalanine mutant adeno-associated virus vectors*

AAV8		
Serotype	*Mutations*	*Expressed gene*
AAV8 WT	(none)	mcherry
AAV8 1M	Y733F	mcherry
AAV8 2M	Y447F+Y733F	mcherry
AAV8 3M	Y275F+Y447F+Y733F	mcherry

AAV, adeno-associated virus; F, phenylalanine; Y, tyrosine.

Injection with double-mutant (2M) and triple-mutant (3M) resulted in 4- and 3.3-fold enhanced mCherry expression in the pancreas as compared to WT-AAV8 (average radiant efficiency 9.48×10^{9} and 7.66×10^{9} respectively, $n=3$ per group, $p<0.05$) (Fig. 1A). In addition, we observed a wide variation of mCherry expression in the liver; however, the difference in the levels of mCherry expression did not statistically differ between AAV8 1M, 2M, and 3M. We also analyzed lung, heart, spleen, and kidney using Xenogen IVIS imaging (Fig. 1A) and only detected a low (<3 %) mCherry transduction efficiency in the kidney (and no signal in lung, heart, and spleen), confirming that AAV8 vectors did not transduce other tissues at high frequency.

To further analyze mCherry fluorescent signal at the cellular level, pancreas and liver tissues were frozen in OCT medium and sectioned using cryostat for fluorescent microscope analysis. Fluorescent images were analyzed by Image J software to determine the percent mCherry expression. Measurement of fluorescence signal from frozen pancreas sections confirmed that 45–70% and 25–60% mCherry expression was achieved in the pancreas following i.p. administration of Y447F+Y733F-AAV8 and Y275F+Y447F+Y733F-AAV8, respectively, whereas only ~7% mCherry expression was obtained in the pancreas with the WT-AAV8 administration (Fig. 1B and Supplementary Fig. S1; Supplementary Data are available online at www.liebertpub.com/hgtb). Importantly, treatment of mice ($n=3$ per group) with double mutant Y447F+Y733F-AAV8 showed 8-fold increased mCherry expression when two independent sections from each animals were analyzed, $p<0.01$ (Fig. 1B) as compared with WT-AAV8, indicating significantly enhanced transduction efficiency in the pancreas. We also observed that i.p. injection of WT-AAV8 and Y447F+Y733F-AAV8 into 2-month-old FVB/C129 mice predominantly transduce exocrine pancreatic tissues; however, Image J analysis performed on the same samples showed 1–5% transduction efficiency of WT-AAV8 and Y447F+Y733F-AAV8 in the endocrine pancreas as previously reported.[23] We observed furthermore

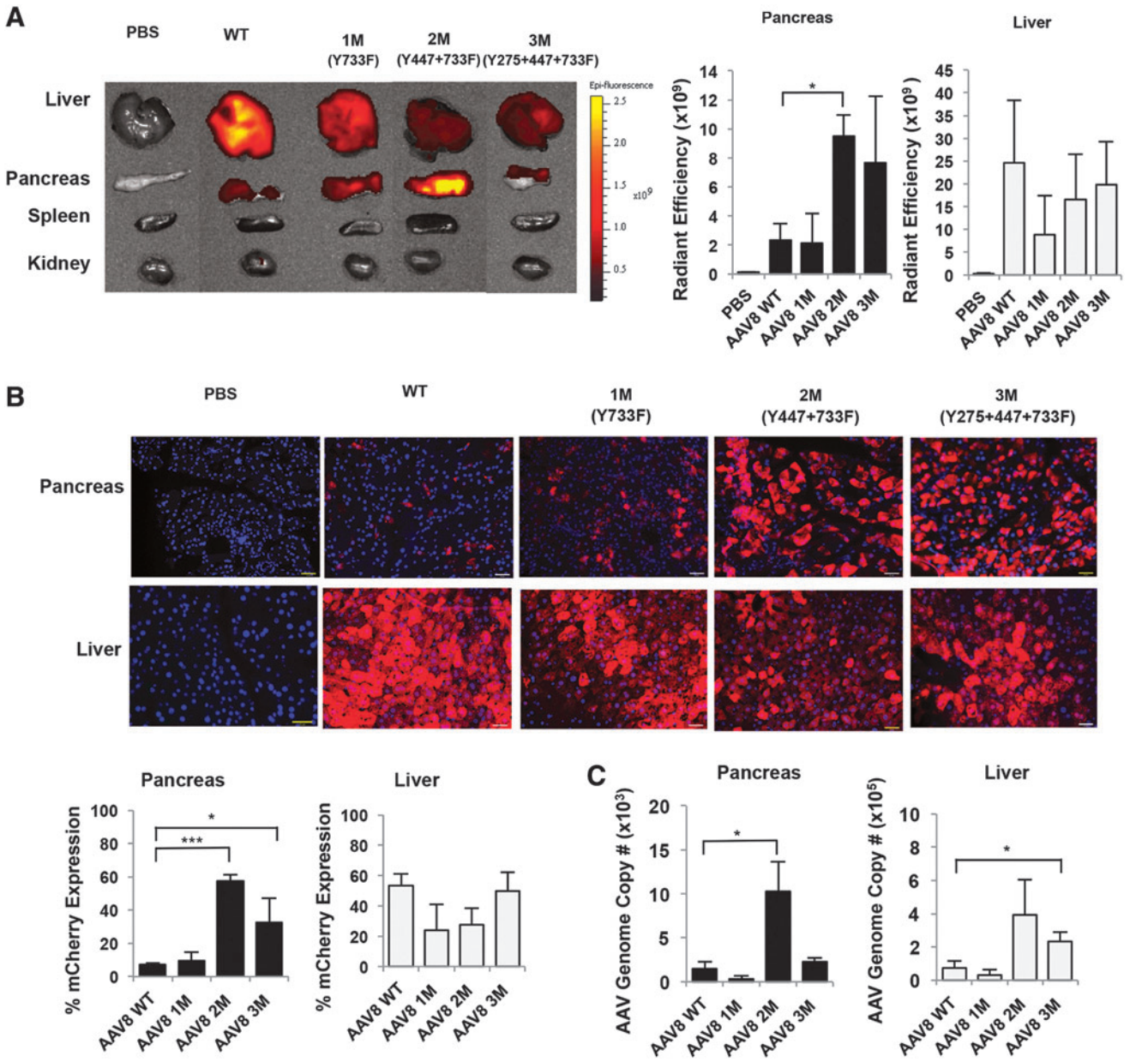

Figure 1. Y447F+Y733F-AAV8 double mutant improves transduction efficiency in mice pancreas. **(A)** *Ex vivo* tissue fluorescence imaging and quantitative analysis of mCherry expression following i.p. injection of AAV8 WT, 1M, 2M, and 3M. Representative image is shown (left panel). Scale bars presented as Radiant Efficiency [(p/s/cm^2/sr)/(μW/cm^2)]. Results are shown as the mean ± SE (right panel) (*$p < 0.1$, $n = 3$ per group). **(B)** Fluorescence image and quantification of percent mCherry expression efficiency in pancreas and liver tissue. Representative images are shown. Blue: DAPI staining for nuclei; red: mCherry expression. Scale bar: 65 μm. Results in the lower panel are shown as the mean ± SE (*$p < 0.1$***, $p < 0.001$, $n = 3$ per group, two sections from each animal were analyzed). **(C)** Quantitative real-time PCR analysis of AAV genomes. Results are shown as the average AAV genome copy number per microgram of total DNA ± SE (*$p < 0.1$, $n = 3$ per group). AAV, adeno-associated virus; F, phenylalanine; i.p., intraperitoneal; M, mutant; SE, standard error; WT, wild type; Y, tyrosine.

that the enhanced transduction efficiency of the double mutant AAV8 correlated well with the increased vector genome copy numbers in the pancreas (Fig. 1B, C). Y447F+Y733F-AAV8 showed a 6.87-fold higher genome copy number as compared with the WT-AAV8 (10,285 vs. 1,500 vector copies/μg DNA respectively, $n = 3$ per group, $p < 0.05$) (Fig. 1C). Mice treated with M3 AAV8 vector showed lower vg copy number and a significant variation of mCherry expression. Therefore, Y447F+Y733F-AAV8 M2 AAV8 was selected for future studies. The AAV vector genome copy number in the liver, however, did not correlate with the mCherry expression for both 2M and 3M AAV8. The AAV vector genome copy number increased 2.5- ~3.5-fold after capsid-optimized mutant AAV8 injection as compared with

WT-AAV8 vector (Fig. 1C), but the mCherry expression in the liver was not enhanced by these two mutant AAV8 vectors (Fig. 1B; Supplementary Fig. S2). A discrepancy between copy number and expression in the liver has been shown previously in whole-body distribution studies,[38,52,53] and we also observed variation in our analysis of liver tissues. In addition, the ubiquitination/proteasome machinery involved in processing the Y-F mutant AAV8 vectors might be different between pancreas and liver, which is consistent with our previously publish results.[54,55] Another possibility is that after i.p. injection of AAV, a substantial amount of mutant AAV vector is sequestered in pancreas; therefore, a relatively lower amount of AAV vector is delivered to liver.

Our results demonstrate that i.p. administration of Y447F+Y733F-AAV8 into mice can significantly enhance mCherry gene expression in the pancreas suggesting that i.p. delivery of AAV8 capsid double mutant is a promising method for gene delivery to the pancreas.

Intraperitoneal delivery of Y447F+Y733F-AAV8 results in higher transduction efficiency in the pancreas compared with tail vein administration

To evaluate the effect of different routes of delivery and AAV-mediated pancreatic transduction, we compared two systemic delivery methods (intraperitoneal [i.p.] and tail vein intravenous [i.v.]) in adult mice. The double-mutant AAV8 was selected for administration because of its high transduction efficiency in the pancreas. Briefly, 1×10^{11} vg/animal of the WT-AAV8 or the Y447F+Y733F-AAV8 were administered to 8-week-old WT mice, either by i.v. or i.p. injection. Two weeks post injection, pancreas and liver tissues were collected to analyze mCherry expression and AAV genome copy number. We found that i.p. delivery of AAV8-WT and Y447F+Y733F-AAV8 increased transduction efficiency in the pancreas as compared with i.v. injection. While i.v. injection of both AAV8-WT and Y447F+Y733F-AAV8 showed relatively low percent mCherry expression in the pancreas (5.25% and 6.25% mCherry efficiency respectively), i.p. injection of AAV8-WT and Y447F+Y733F-AAV8 increased percent mCherry expression efficiency 4.28- to 9.6-fold respectively (Fig. 2A, 22.5% mCherry expression efficiency for AAV8-WT, 60% mCherry expression efficiency for Y447F+Y733F-AAV8, $n=3$ per group, $p<0.05$). In addition, we found that AAV8 vector genome copy number in the pancreas correlated with mCherry expression levels. Intraperitoneal injection of WT-AAV8 and Y447F+Y733F-AAV8 showed a 32.18-fold to 103.45-fold increase respectively compared with i.v administration (WT-AAV8 i.p. 5,793 vs. i.v.180 copies/μg, $n=3$ per group, $p<0.05$ and Y447F+Y733F-AAV8 i.p. injection 15,311 vs. i.v. 148 copies/μg DNA, $n=3$ per group, $p<0.05$) (Fig. 2B). No significant differences were observed in the mCherry gene expression or AAV8 vector genome copy number in the liver between i.v. versus i.p. injected mice (Fig. 2A, B). WT-AAV8 genome copy number detected in the liver was similar or slightly higher in our experiment as compared to previously published reports.[52,56,57] Thus, we observed enhanced efficiency in the pancreas, but not in the liver, when comparing the i.p. versus i.v. routes of injection (Fig. 2A, B). Taken together, these data demonstrate that systemic i.p. administration of the AAV8 results in significant enhancement of transduction efficiency in the pancreas as compared with the i.v. injection. These data also demonstrate that higher efficiency transduction of the pancreas can be achieved by i.p. injection of Y447F+Y733F-AAV8 vectors at a 3-fold lower dose (1×10^{11} vg/animal) as compared with the previously published dosages ($3–5\times10^{11}$ vg/animal of AAV8 vectors).[22]

Y447F+Y733F-AAV8 efficiently transduce mouse pancreatic ductal adenocarcinomas in $Kras^{G12D+/-}$ and $Kras^{G12D/+}$/$PTEN^{+/-}$ mice

Since we observed increased transduction efficiency of Y447F+Y733F-AAV8 in the pancreas by i.p. injections in the WT mice, we next examined whether Y447F+Y733F-AAV8 could also transduce mouse pancreatic ductal adenocarcinomas (PDAC) in genetically engineered $Kras^{G12D/+}$/$Pten^{+/-}$ and $Kras^{G12D/+}$mice.[44] These $Kras^{G12D/+}$/$Pten^{+/-}$ and $Kras^{G12D/+}$ mice models develop spontaneous PDAC closely recapitulating human pancreatic carcinoma with a median survival of $\sim$3.5 and $\sim$6.8 months respectively.[44] We injected the WT-AAV8 ($n=2$) or Y447F+Y733F-AAV8 ($n=2$) into 2.3- and 2.8-month-old $Kras^{G12D/+}$/$Pten^{+/-}$ or 5-month-old $Kras^{G12D/+}$ mice. Each mouse was i.p. injected with $3x10^{11}$ vg/animal using the WT- or Y447F+Y733F-AAV8. Two weeks after injection, mouse pancreatic tumors were excised and tumor histology, percent of mCherry expression, and viral genome copy numbers were analyzed. At this time point, all genetically engineered mice exhibited high-grade pancreatic cancer (PDAC grade 2–3) as determined by veterinary pathologist (Fig. 3A). We examined six independent tissue sections for each of the individual mice and found that i.p. administration of Y447F+Y733F-AAV8 enhanced mCherry expression in mouse PDAC as compared with the WT-AAV8 injection (21.6% vs. 6.75 % respectively; Fig. 3B, C). In addition, AAV8 vector genome copy numbers

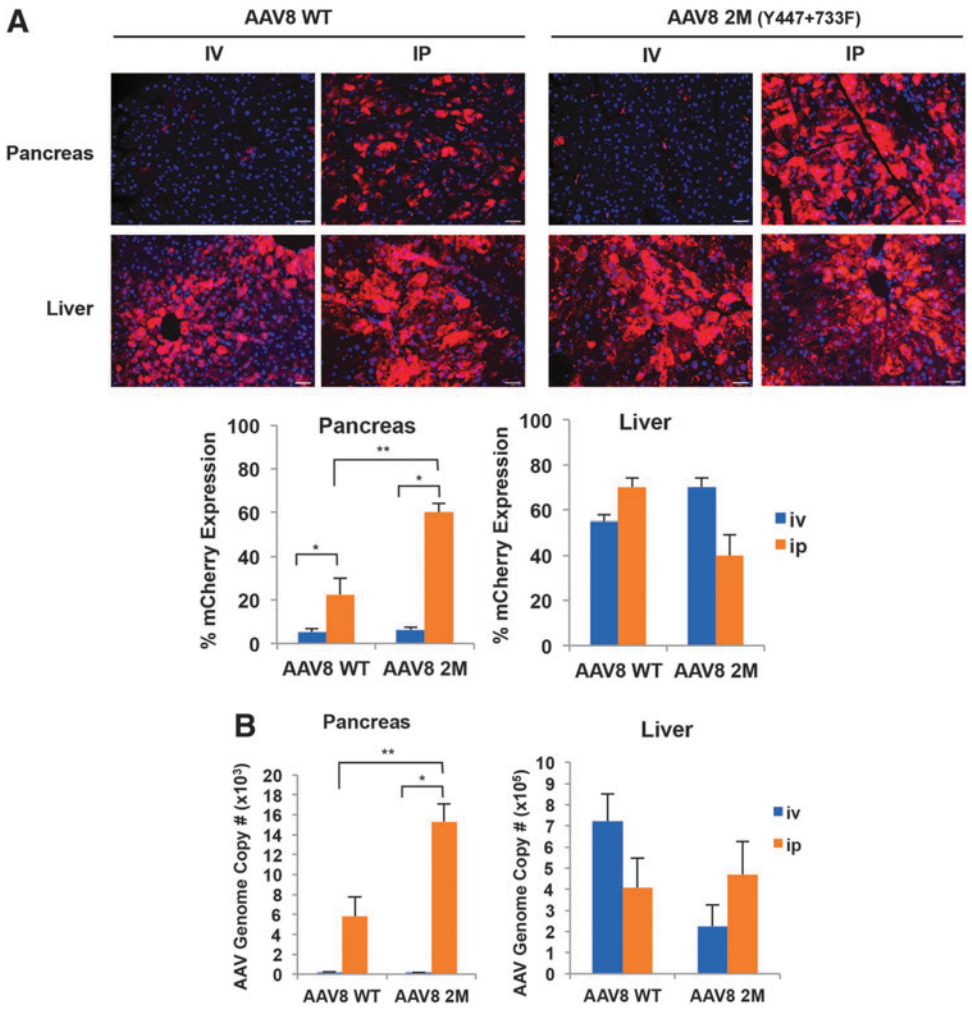

Figure 2. Intraperitoneal administration of Y447F+Y733F-AAV8 allows for a greater transduction efficiency and gene expression in the pancreas than tail vein (i.v.) injection. **(A)** Fluorescence imaging and quantification of percent mCherry expression efficiency in pancreas and liver tissues. Two-month-old mice were injected either i.v. or i.p. with 1×10^{11} vg/animal of WT-AAV8 or Y447F+Y733F-AAV8, both encoding mCherry gene. Blue: DAPI staining for nuclei; red: mCherry expression. Scale bar: 65 μm. Quantative mCherry expression are shown as the mean ± SE (*p < 0.1, **$p < 0.01$, $n = 3$ per group) **(B)** Quantitative real-time PCR analysis for AAV genome. Results are shown as the average AAV genome copy number per μg of total DNA ± SE (*$p < 0.1$, $n = 3$ per group). i.v., intravenous (tail vein); vg, viral genomes.

following Y447F+Y733F-AAV8 injection was 12.3-folds higher than with WT-AAV8 administration into PDAC mice (26,575 vs. 2,165 vector copies/μg gDNA, $n = 2$ per group) (Fig. 3D). Thus, the studies described here suggest that is now feasible to achieve high-efficiency transduction of both normal and malignant pancreatic tissues following i.p. administration of capsid-optimized AAV8, which has implications in the use of these vectors in the potential gene therapy of pancreatic diseases in general, and PDAC in particular.

DISCUSSION

Recombinant AAV (rAAV) vectors have gained significant attention due to their low-immunogenicity and their ability to mediate high-efficiency transduction and sustained transgene expression with non-pathogenic effects after decades of work with small and large animal models.[13,24] The safety and efficacy of rAAV in a number of phase 1–3 clinical trials in humans has also been firmly established.[39,58] More specifically, the use of AAV8 has led to long-term expression and phenotypic correction of Factor IX in patients with hemophilia B.[58] Although AAV8 have been used in preclinical animal models for the potential treatment of PDAC, only a modest level of transduction efficiency in the pancreas has been achieved.[21–25] We reasoned that this drawback could potentially be overcome by the use of a new capsid-optimized AAV8 vector. In our efforts to identify the most efficient Y-F mutant AAV8 vector to target normal pancreas or PDAC, we investigated three AAV8 capsid mutants (Y733F, Y447F+Y733F, and

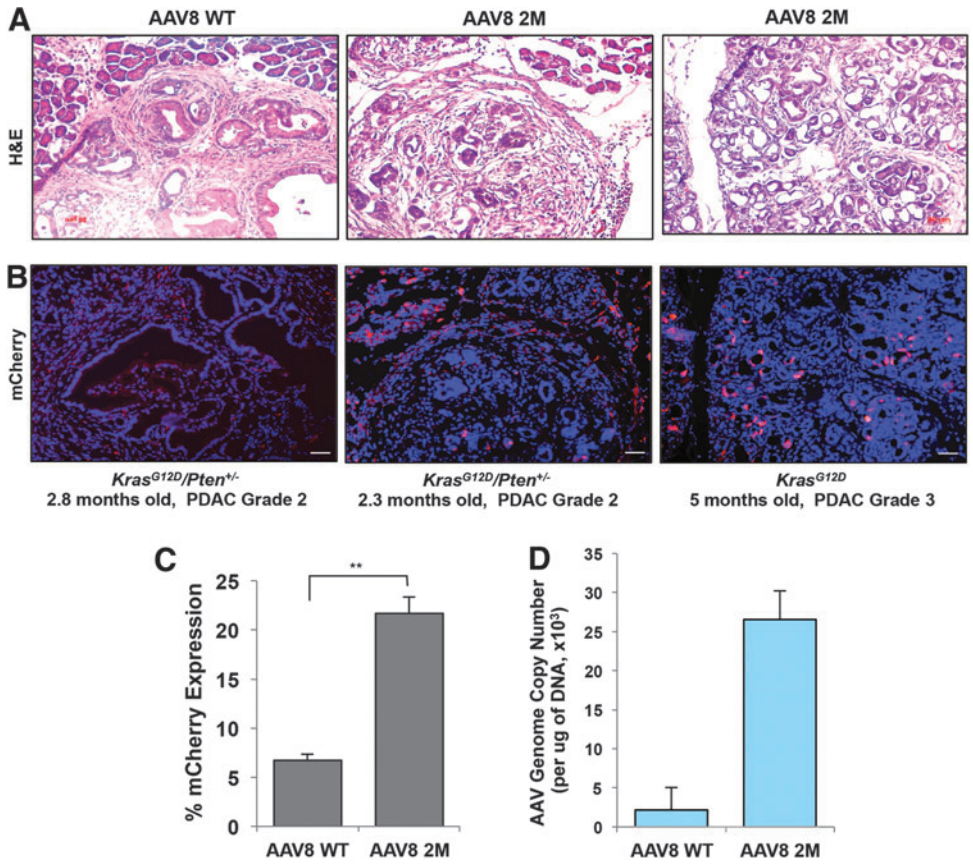

Figure 3. Y447F+Y733F-AAV8 efficiently transduces mouse pancreatic ductal adenocarcinomas in $Kras^{G12D+/-}$ and $Kras^{G12D/+}/PTEN^{+/-}$ genetically engineered mice. **(A)** Haemotoxylin and eosin staining of mouse PDAC. **(B)** Expression of mCherry in PDAC under fluorescence microscopy. Blue: DAPI staining for nucleus; red: mCherry expression. Scale bar: 65 μm. **(C)** Quantification of percent mCherry expression efficiency in PDAC. Results are shown as the mean ± SE (**$p<0.01$, $n=2$ per group, three sections from each animal were analyzed). **(D)** Quantitative analysis of viral genome copy number by real-time PCR. Results are shown as the mean ± SE ($n=2$ per group). PDAC, pancreatic ductal adenocarcinoma.

Y275F+Y447F+Y733F) and compared their efficiency with the WT-AAV8. We observed that the Y447F+Y733F double-mutant AAV8 is capable of efficient delivery with transgene expression in mouse pancreatic tissues *in vivo* following i.p. administration.

In addition, we observed that the route of AAV administration substantially influences pancreas transduction efficiency *in vivo*. For example, local delivery methods such as intrapancreatically,[23,24] intraductally,[21,25] or through the intrapancreatic vessels[26] are more efficient than systemic administration.[21,22] Interestingly, i.p. injection of AAV8 has previously been shown to transduce pancreatic cells more efficiently than tail-vein injection,[22] and i.p. delivery of an AAV8 vector encoding interleukin-2 has been proposed as an attractive gene therapeutic to prevent progress of diabetes *in vivo*.[59] However, the efficiency of transgene expression in the pancreas is still suboptimal. When we compared two different systemic delivery routes (i.p. vs. i.v.), we observed that i.p. administrations of the Y447F+Y733F double-mutant AAV8 efficiently enhanced mCherry expression and viral gene transfer (as demonstrated by viral genome copy number) in the pancreas as compared to i.v. administration. Our data demonstrate that i.p. injection of capsid-optimized AAV8 (Y447F+Y733F-AAV8) shows significant increase of transduction efficiency in the pancreas even at a ~10-fold lower dose than previously reported for intraductal or i.v. WT-AAV8 administration.[21] Thus, we have determined that i.p. delivery of the Y447F+Y733F-AAV8 vector is the best systemic strategy to deliver therapeutic genes to the pancreas *in vivo*.

Although previous studies have documented that AAV8 serotype vectors possess a broad tissue tropism, these vectors predominantly transduce the mouse liver compared to other tissues following i.v. delivery.[60,61] In contrast, we have now observed that i.p. delivery of the Y447F+Y733F-AAV8 capsid mutant resulted in a significant enhancement in the transduction efficiency in the pancreas while transduction efficiency in the liver was observed

over a variable range following i.p. administration. These data are consistent with our recently published studies,[62] suggesting that the ubiquitination/proteasome machinery involved in processing the Y-F mutant AAV8 vectors might be different between pancreas and liver, and that the use of lower dose of Y447F+Y733F-AAV8 might also minimize undesired host immune responses to the WT-AAV8 vectors, as has been occasionally observed in human clinical trial.[20,58] Prior whole body distribution studies have observed a discrepancy between the AAV vg copy number and overall gene expression delivered by AAV vectors.[38,52,53] We also observed a similar discrepancy between vg copy number and mCherry expression levels which cannot be solely explained by delivery efficiency since AAV infection is a complex, multiple-step process involving cell entry, intracellular trafficking, nuclear translocation, and uncoating.[63] For example, we previously showed that capsid-optimized AAV vectors are more efficient in escaping protein degradation than WT vectors resulting in more vg accumulating in the nucleus within several days after infection.[54,55] In addition, despite the selection of a ubiquitous promoter, we still expect an impact of mCherry expression depending on tissue types including normal or malignant liver and pancreas.

Our previously published studies with the capsid-optimized AAV2 showed that the transduction efficiency of a Y-F triple-mutant was significantly higher than that of the individual single- or double-mutants.[30] In contrast, this study shows that the transduction efficiency of the Y-F triple-mutant AAV8 was not further enhanced compared with the Y-F double-mutant AAV8 vector. Although the molecular mechanism underlying this observation remains unknown, varying levels of enhanced transduction efficiencies by single, double, triple, or quadruple Y-F mutants of various AAV serotypes have previously been reported using different cells and tissues.[30–32,45,54] Therefore, the optimal viral capsid mutant can be identified only following direct testing.

We have now studied a genetically engineered mouse animal model of pancreatic ductal adenocarcinoma to evaluate and optimize gene transfer into pancreatic exocrine cells. The high transduction efficiency of Y447F+Y733F-AAV8 into pancreatic tumors may allow future use of Y447F+Y733F-AAV8 as a delivery tool to test the effect of modulating gene expression on pancreatic microenvironment and host immune response. It remains to be determined whetherAAV transgene may integrate into host genome and persist in rapidly dividing tumor cells to affect a higher percentage of these cells. This work will also allow studies to further enhance specificity and efficiency into pancreatic tumor cells.

In conclusion, we observed that the Y447F+Y733F double-mutant AAV8 serotype shows efficient delivery and transgene expression in normal pancreas and pancreatic tumor tissues following i.p. administration. Future studies will evaluate the safety and efficacy of this capsid-optimized AAV8 for therapeutic gene delivery and shRNA delivery to target genes that play a role in pancreatic diseases such as PDAC.

ACKNOWLEDGMENTS

We thank Dr. Stanley Lin for a critical review of this manuscript. This work was supported in part by Public Health Service grants R01 HL-097088, R21 EB-015684 (to A.S.), P30 EY021721 (to W.W.H.), R01 CA-188132 (to M.Z-K.) from the National Institutes of Health, the Gatorade Trust through funds distributed by the University of Florida, Department of Medicine (to M.Z-K. and F.J.K.), UF Health Cancer Center Team Science Project grant (to M.Z-K.) and James and Esther King grant 5JK04 from Florida Department of Health (to F.J.K. and M.Z-K.)

AUTHOR DISCLOSURE

Min Chen, Kyungah Maeng, Akbar Nawab, Rony A. Francois, Julie K. Bray, Mary K. Reinhard, Sanford L. Boye, Georgiy Aslanidi, Frederic J. Kaye, and Maria Zajac-Kaye have no competing financial interests. William W. Hauswirth and the University of Florida have a financial interest in the use of AAV therapies and own equity in a company (AGTC Inc.) that might, in the future, commercialize some aspects of this work. Arun Srivastava holds issued patents related to AAV vectors that have been licensed to various AAV gene therapy companies.

REFERENCES

1. Geer RJ, Brennan MF. Prognostic indicators for survival after resection of pancreatic adenocarcinoma. Am J Surg 1993;165:68–72; discussion 72–63.
2. Williamson RC. Pancreatic cancer: the greatest oncological challenge. Br Med J (Clin Res Ed) 1988;296:445–446.
3. Bekaii-Saab T, Goldberg R. Therapeutic advances in pancreatic cancer: miles to go before we sleep. J Natl Cancer Inst 2015;107.
4. Paniccia A, Hosokawa P, Henderson W et al. Characteristics of 10-year survivors of pancreatic ductal adenocarcinoma. JAMA Surg 2015;150:701–710.
5. Ryan DP, Hong TS, Bardeesy N. Pancreatic adenocarcinoma. N Engl J Med 2014;371:1039–1049.
6. Ucar DA, Hochwald SN. FAK and interacting proteins as therapeutic targets in pancreatic cancer. Anticancer Agents Med Chem 2010;10:742–746.

7. Zheng D, Golubovskaya V, Kurenova E et al. A novel strategy to inhibit FAK and IGF-1R decreases growth of pancreatic cancer xenografts. Mol Carcinog 2010;49:200–209.
8. Noro T, Miyake K, Suzuki-Miyake N et al. Adeno-associated viral vector-mediated expression of endostatin inhibits tumor growth and metastasis in an orthotropic pancreatic cancer model in hamsters. Cancer Res 2004;64:7486–7490.
9. Zhang K, Jiao X, Liu X et al. Knockdown of snail sensitizes pancreatic cancer cells to chemotherapeutic agents and irradiation. Int J Mol Sci 2010; 11:4891–4892.
10. Daya S, Berns KI. Gene therapy using adeno-associated virus vectors. Clin Microbiol Rev 2008; 21:583–593.
11. Ponnazhagan S, Curiel DT, Shaw DR et al. Adeno-associated virus for cancer gene therapy. Cancer Res 2001;61:6313–6321.
12. Srivastava A. Adeno-associated virus-mediated gene transfer. J Cell Biochem 2008;105:17–24.
13. Mueller C, Flotte TR. Clinical gene therapy using recombinant adeno-associated virus vectors. Gene Ther 2008;15:858–863.
14. High KA, Aubourg P. rAAV human trial experience. Methods Mol Biol 2011;807:429–457.
15. Davidoff AM, Gray JT, Ng CY et al. Comparison of the ability of adeno-associated viral vectors pseudotyped with serotype 2, 5, and 8 capsid proteins to mediate efficient transduction of the liver in murine and nonhuman primate models. Mol Ther 2005;11:875–888.
16. Boutin S, Monteilhet V, Veron P et al. Prevalence of serum IgG and neutralizing factors against adeno-associated virus (AAV) types 1, 2, 5, 6, 8, and 9 in the healthy population: implications for gene therapy using AAV vectors. Hum Gene Ther 2010;21:704–712.
17. Gao GP, Alvira MR, Wang L et al. Novel adeno-associated viruses from rhesus monkeys as vectors for human gene therapy. Proc Natl Acad Sci U S A 2002;99:11854–11859.
18. Chandler RJ, Tarasenko TN, Cusmano-Ozog K et al. Liver-directed adeno-associated virus serotype 8 gene transfer rescues a lethal murine model of citrullinemia type 1. Gene Ther 2013;20:1188–1191.
19. Wang Z, Zhu T, Qiao C et al. Adeno-associated virus serotype 8 efficiently delivers genes to muscle and heart. Nat Biotechnol 2005;23:321–328.
20. Nathwani AC, Tuddenham EG, Rangarajan S et al. Adenovirus-associated virus vector-mediated gene transfer in hemophilia B. N Engl J Med 2011;365: 2357–2365.
21. Jimenez V, Ayuso E, Mallol C et al. *In vivo* genetic engineering of murine pancreatic beta cells mediated by single-stranded adeno-associated viral vectors of serotypes 6, 8 and 9. Diabetologia 2011; 54:1075–1086.
22. Wang Z, Zhu T, Rehman KK et al. Widespread and stable pancreatic gene transfer by adeno-associated virus vectors via different routes. Diabetes 2006;55: 875–884.
23. Cheng H, Wolfe SH, Valencia V et al. Efficient and persistent transduction of exocrine and endocrine pancreas by adeno-associated virus type 8. J Biomed Sci 2007;14:585–594.
24. Wang AY, Peng PD, Ehrhardt A et al. Comparison of adenoviral and adeno-associated viral vectors for pancreatic gene delivery *in vivo*. Hum Gene Ther 2004;15:405–413.
25. Loiler SA, Tang Q, Clarke T et al. Localized gene expression following administration of adeno-associated viral vectors via pancreatic ducts. Mol Ther 2005;12:519–527.
26. Maione F, Molla F, Meda C et al. Semaphorin 3A is an endogenous angiogenesis inhibitor that blocks tumor growth and normalizes tumor vasculature in transgenic mouse models. J Clin Invest 2009;119: 3356–3372.
27. Mingozzi F, High KA. Therapeutic *in vivo* gene transfer for genetic disease using AAV: progress and challenges. Nat Rev Genet 2011;12:341–355.
28. Mendell JR, Rodino-Klapac L, Sahenk Z et al. Gene therapy for muscular dystrophy: lessons learned and path forward. Neurosci Lett 2012; 527:90–99.
29. Zhong L, Li B, Jayandharan G et al. Tyrosine-phosphorylation of AAV2 vectors and its consequences on viral intracellular trafficking and transgene expression. Virology 2008;381:194–202.
30. Zhong L, Li B, Mah CS et al. Next generation of adeno-associated virus 2 vectors: point mutations in tyrosines lead to high-efficiency transduction at lower doses. Proc Natl Acad Sci U S A 2008; 105:7827–7832.
31. Song L, Li X, Jayandharan GR et al. High-efficiency transduction of primary human hematopoietic stem cells and erythroid lineage-restricted expression by optimized AAV6 serotype vectors *in vitro* and in a murine xenograft model *in vivo*. PLoS One 2013;8: e58757.
32. Petrs-Silva H, Dinculescu A, Li Q et al. Novel properties of tyrosine-mutant AAV2 vectors in the mouse retina. Mol Ther 2011;19:293–301.
33. Martini SV, da Silva AL, Ferreira D et al. Single tyrosine mutation in AAV8 vector capsid enhances gene lung delivery and does not alter lung morphofunction in mice. Cell Physiol Biochem 2014; 34:681–690.
34. Mowat FM, Gornik KR, Dinculescu A et al. Tyrosine capsid-mutant AAV vectors for gene delivery to the canine retina from a subretinal or intravitreal approach. Gene Ther 2014;21:96–105.
35. Pang JJ, Dai X, Boye SE et al. Long-term retinal function and structure rescue using capsid mutant AAV8 vector in the rd10 mouse, a model of recessive retinitis pigmentosa. Mol Ther 2011;19: 234–242.
36. Markusic DM, Herzog RW, Aslanidi GV et al. High-efficiency transduction and correction of murine hemophilia B using AAV2 vectors devoid of multiple surface-exposed tyrosines. Mol Ther 2010;18: 2048–2056.
37. Ojano-Dirain C, Glushakova LG, Zhong L et al. An animal model of PDH deficiency using AAV8-siRNA vector-mediated knockdown of pyruvate dehydrogenase E1alpha. Mol Genet Metab 2010;101:183–191.
38. Li S, Ling C, Zhong L et al. Efficient and Targeted Transduction of Nonhuman Primate Liver With Systemically Delivered Optimized AAV3B Vectors. Mol Ther 2015;23:1867–1876.
39. Feuer WJ, Schiffman JC, Davis JL et al. Gene Therapy for Leber Hereditary Optic Neuropathy: Initial Results. Ophthalmology 2016;123:558–570.
40. Petrs-Silva H, Dinculescu A, Li Q et al. High-efficiency transduction of the mouse retina by tyrosine-mutant AAV serotype vectors. Mol Ther 2009;17:463–471.
41. Ryals RC, Boye SL, Dinculescu A et al. Quantifying transduction efficiencies of unmodified and tyrosine capsid mutant AAV vectors *in vitro* using two ocular cell lines. Mol Vis 2011;17:1090–1102.
42. Zolotukhin S, Potter M, Zolotukhin I et al. Production and purification of serotype 1, 2, and 5 recombinant adeno-associated viral vectors. Methods 2002;28:158–167.
43. Aslanidi G, Lamb K, Zolotukhin S. An inducible system for highly efficient production of recombinant adeno-associated virus (rAAV) vectors in insect Sf9 cells. Proc Natl Acad Sci U S A 2009; 106:5059–5064.
44. Hill R, Calvopina JH, Kim C et al. PTEN loss accelerates KrasG12D-induced pancreatic cancer development. Cancer Res 2010;70:7114–7124.
45. Kauss MA, Smith LJ, Zhong L et al. Enhanced long-term transduction and multilineage engraftment of human hematopoietic stem cells transduced with tyrosine-modified recombinant adeno-associated virus serotype 2. Hum Gene Ther 2010;21:1129–1136.
46. Cheng B, Ling C, Dai Y et al. Development of optimized AAV3 serotype vectors: mechanism of high-efficiency transduction of human liver cancer cells. Gene Ther 2012;19:375–384.
47. de Backer MW, Brans MA, Luijendijk MC et al. Optimization of adeno-associated viral vector-mediated gene delivery to the hypothalamus. Hum Gene Ther 2010;21:673–682.
48. Kay CN, Ryals RC, Aslanidi GV et al. Targeting photoreceptors via intravitreal delivery using novel, capsid-mutated AAV vectors. PLoS One 2013;8:e62097.
49. Rehman KK, Wang Z, Bottino R et al. Efficient gene delivery to human and rodent islets with double-stranded (ds) AAV-based vectors. Gene Ther 2005; 12:1313–1323.
50. McCarty DM. Self-complementary AAV vectors; advances and applications. Mol Ther 2008;16:1648–1656.
51. Buie LK, Rasmussen CA, Porterfield EC et al. Self-complementary AAV virus (scAAV) safe and long-term gene transfer in the trabecular meshwork of

living rats and monkeys. Invest Ophthalmol Vis Sci 2010;51:236–248.

52. Zincarelli C, Soltys S, Rengo G et al. Analysis of AAV serotypes 1–9 mediated gene expression and tropism in mice after systemic injection. Mol Ther 2008;16:1073–1080.
53. Grimm D, Pandey K, Nakai H et al. Liver transduction with recombinant adeno-associated virus is primarily restricted by capsid serotype not vector genotype. J Virol 2006;80:426–439.
54. Aslanidi GV, Rivers AE, Ortiz L et al. Optimization of the capsid of recombinant adeno-associated virus 2 (AAV2) vectors: the final threshold? PLoS One 2013;8:e59142.
55. Pandya J, Ortiz L, Ling C et al. Rationally designed capsid and transgene cassette of AAV6 vectors for dendritic cell-based cancer immunotherapy. Immunol Cell Biol 2014;92:116–123.
56. Michelfelder S, Varadi K, Raupp C et al. Peptide ligands incorporated into the threefold spike capsid domain to re-direct gene transduction of AAV8 and AAV9 *in vivo*. PLoS One 2011;6:e23101.
57. Yasuda M, Bishop DF, Fowkes M et al. AAV8-mediated gene therapy prevents induced biochemical attacks of acute intermittent porphyria and improves neuromotor function. Mol Ther 2010;18:17–22.
58. Nathwani AC, Reiss UM, Tuddenham EG et al. Long-term safety and efficacy of factor IX gene therapy in hemophilia B. N Engl J Med 2014;371:1994–2004.
59. Flores RR, Zhou L, Robbins PD. Expression of IL-2 in beta cells by AAV8 gene transfer in pre-diabetic NOD mice prevents diabetes through activation of FoxP3-positive regulatory T cells. Gene Ther 2014;21:715–722.
60. Nakai H, Fuess S, Storm TA et al. Unrestricted hepatocyte transduction with adeno-associated virus serotype 8 vectors in mice. J Virol 2005;79:214–224.
61. Sarkar R, Tetreault R, Gao G et al. Total correction of hemophilia A mice with canine FVIII using an AAV 8 serotype. Blood 2004;103:1253–1260.
62. Li B, Ma W, Ling C et al. Site-directed mutagenesis of surface-exposed lysine residues leads to improved transduction by AAV2, but not AAV8, vectors in murine hepatocytes *in vivo*. Hum Gene Ther Methods 2015;26:211–220.
63. Harbison CE, Chiorini JA, Parrish CR. The parvovirus capsid odyssey: from the cell surface to the nucleus. Trends Microbiol 2008;16:208–214.

Received for publication June 15, 2016;
accepted after revision January 19, 2017.

Published online: January 25, 2017.